

Supporting Information

Efficient Yolk-shelled Fe-N-C Oxygen Reduction Electrocatalyst via N-rich Molecular Guiding Pyrolysis

Qingxue Lai,^{1*} Hongmei Zheng,¹ Wanying Zhang,¹ Yi Sheng,¹ Luanjie Nie,² Jing Zheng²

¹Jiangsu key Laboratory of Electrochemical Energy Storage Technologies, College of Materials Science and Technologies, Nanjing University of Aeronautics and Astronautics, Nanjing 210016, P. R. China

²Department of Chemistry and Materials Science, College of Science, Nanjing Forestry University, Nanjing 210037, P. R. China

*Corresponding authors: laiqingxue@126.com (Q. Lai);

List and contents

Figure S1. TEM image of FeNC@PM Under a wide field of view.

Figure S2. XPS survey spectra of prepared Fe-N-C materials.

Figure S3. CV curves of prepared Fe-N-C materials with the 30% Pt/C for reference in the O₂-saturated electrolyte.

Figure S4. LSV curves of FeNC@PM materials obtained at different pyrolysis temperatures.

Figure S5. H₂O₂ yield of prepared Fe-N-C materials with the 30% Pt/C for reference

Figure S6. linear fit of capacitive ΔJ/2 vs. scan rates for FeNC@PM materials obtained at different pyrolysis temperatures.

Figure S7. Comparison of the linear fit of capacitive ΔJ/2 vs. scan rates for FeNC@PM materials obtained at 950°C before and after ADT.

Table S1. Contents of different elements in FeNC@PM, FeNC@P, FeNC@M and FeNC from XPS spectra.

Table S2. The content of the different N configuration in the high-resolution N 1s XPS spectra for FeNC@PM, FeNC@P, FeNC@M and FeNC.

Table S3. The content of the different typed carbon structure from Raman spectra

Table S4. ORR activity comparison of previously reported Fe-N-C catalysts with this work in acidic media.

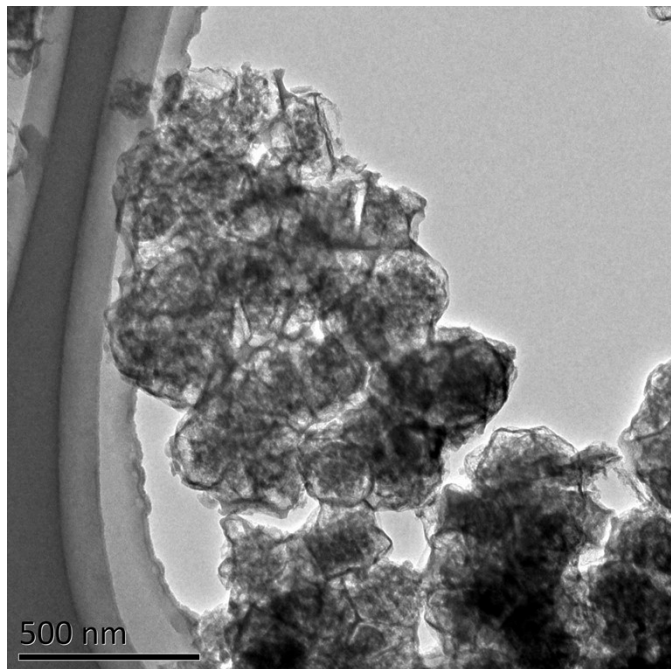


Figure S1. TEM image of FeNC@PM Under a wide field of view.

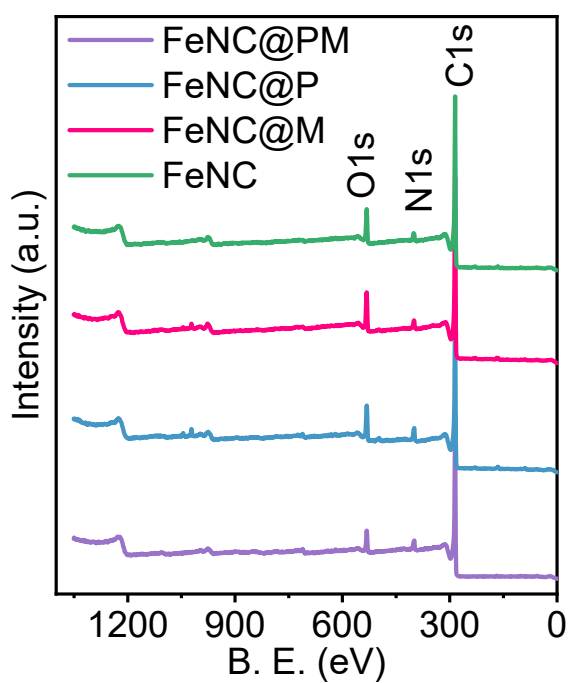


Figure S2. XPS survey spectra of prepared Fe-N-C materials.

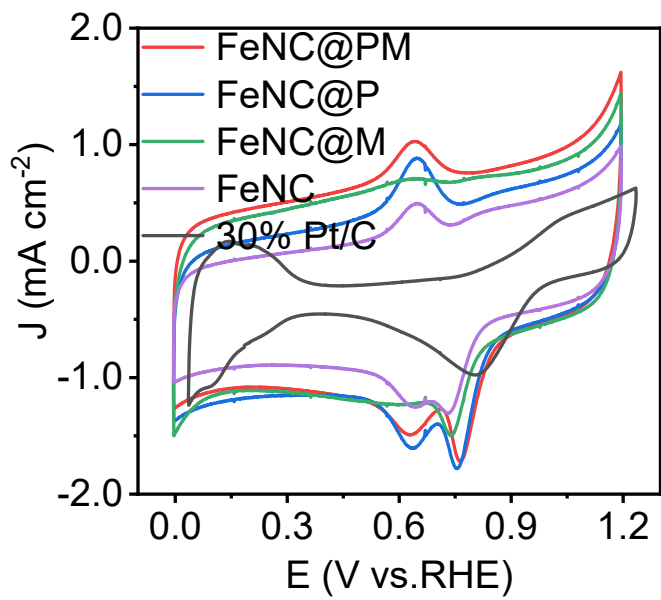


Figure S3. CV curves of prepared Fe-N-C materials with the 30% Pt/C for reference in the O_2 -saturated electrolyte.

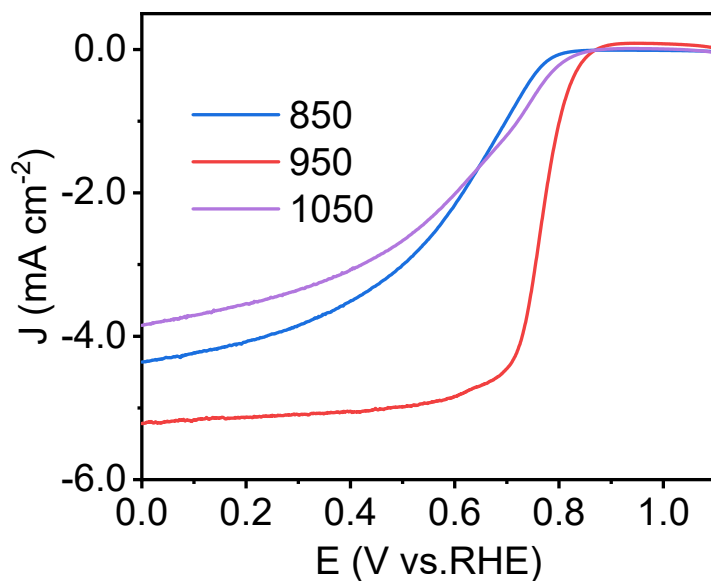


Figure S4. LSV curves of FeNC@PM materials obtained at different pyrolysis temperatures.

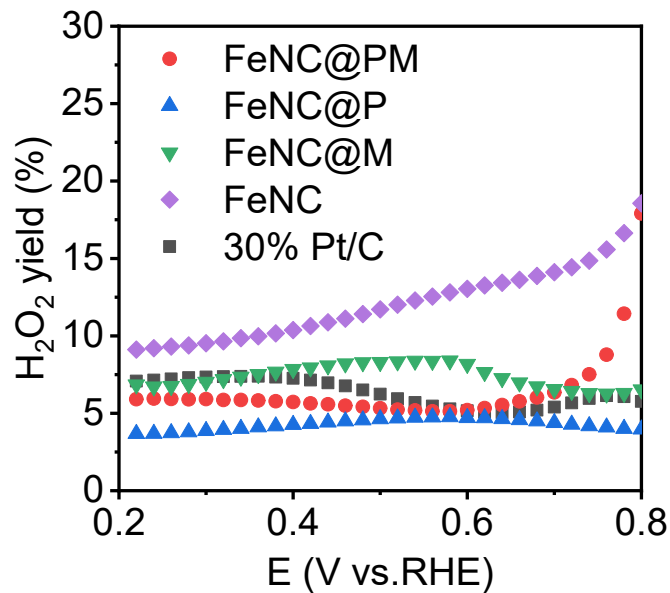


Figure S5. H₂O₂ yield of prepared Fe-N-C materials with the 30% Pt/C for reference

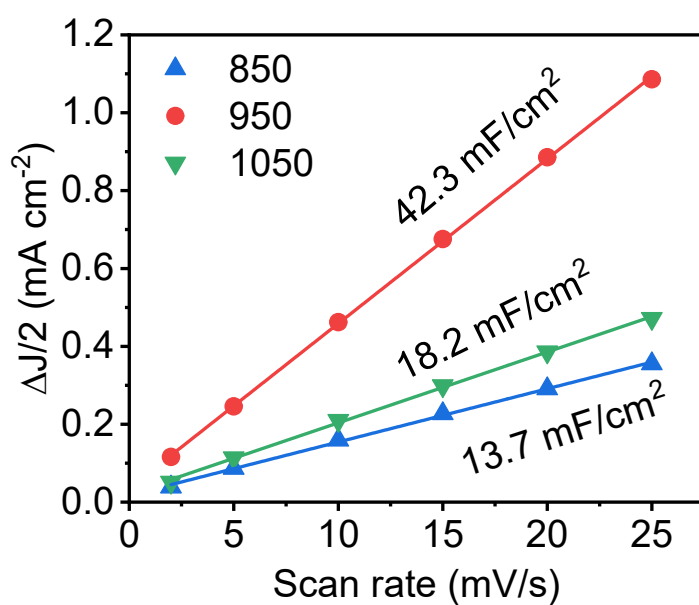


Figure S6. linear fit of capacitive $\Delta J/2$ vs. scan rates for FeNC@PM materials obtained at different pyrolysis temperatures.

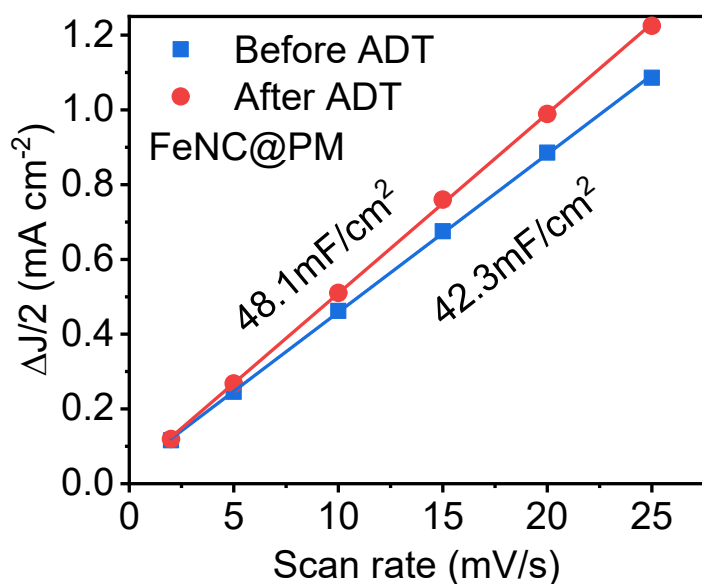


Figure S7. Comparison of the linear fit of capacitive $\Delta J/2$ vs. scan rates for FeNC@PM materials obtained at 950°C before and after ADT.

Table S1. Contents of different elements in FeNC@PM, FeNC@P, FeNC@M and FeNC from XPS spectra.

Sample	C (at.%)	N (at.%)	O (at.%)	Fe (at.%)	Zn (at.%)
FeNC@PM	86.62	5.89	6.46	1.02	-
FeNC@P	79.73	6.15	9.12	0.44	5.56
FeNC@M	84.60	4.48	10.15	0.45	0.33
FeNC	85.49	4.17	9.76	0.58	-

Table S2. The content of the different N configuration in the high-resolution N 1s XPS spectra for FeNC@PM, FeNC@P, FeNC@M and FeNC.

Sample	N1(%)	N2(%)	N3(%)	N4(%)	N5(%)	N6(%)
FeNC@PM	16.9	24.5	7.4	34.1	11.5	5.6
FeNC@P	19.3	23.5	9.7	24.6	4.4	18.5
FeNC@M	10.3	16.9	24.55	30.1	6.2	12.0
FeNC	14.2	14.1	18.8	30.8	7.0	15.1

Table S3. The content of the different typed carbon structure from Raman spectra.

Sample	D (%)	D" (%)	T (%)	G (%)	AD/AG
FeNC@PM	21.6	30.0	36.0	12.4	7.06
FeNC@P	44.2	14.4	15.9	25.5	2.92
FeNC@M	44.1	15.0	21.2	19.7	4.08

Table S4. ORR activity comparison of previously reported Fe-N-C catalysts with this work in acidic media.

	Catalyst	Mass loading (mg/cm ²)	E _{1/2} (V vs. RHE)	J _L (mA/cm ²) @1600 rpm	n	Ref.
1	pyrolyzed Fe-N-C	0.60	~0.755	3.64 (900 rpm)	~3.95	<i>ACS Catal.</i> , 2014, 4, 3928–3936
2	CNT/PC (with Fe-N _x)	0.60	0.79	6.0	--	<i>J. Am. Chem. Soc.</i> , 2016, 138, 15046-5056
3	Fe-CB@PAN-1000	0.80	0.758	4.68 (900 rpm)	3.9	<i>J. Colloid Interface Sci.</i> , 2017, 502, 44-51
4	(Fe,Co)/N-C	1.095	0.863	~6.0	~4.0	<i>J. Am. Chem. Soc.</i> , 2017, 139, 17281-7284
5	Fe/SNC	0.61	0.77	4.8	3.9	<i>Angew. Chem. Int. Ed.</i> , 2017, 56, 13800-13804
6	Fe-N-C	0.24	0.657	4.5	3.99	<i>Int. J. Hydrogen Energy</i> , 2019, 44, 27379-27389
7	P-FeMOF@ZIF-8	0.255	0.73	~5.3	~3.85	<i>ACS Appl. Mater. Interfaces</i> , 2019, 11, 35755–35763
8	Fe-C-N950	~1.0	0.80	~4.0	~4	<i>J. Am. Chem. Soc.</i> , 2020, 142, 12, 5477-5481
9	FeNi0.25-NC	0.60	0.79	5.6	~3.99	<i>Appl. Surf. Sci.</i> , 2021, 538, 148017
10	0.14Co0.01Fe-CB	0.613	0.76	~5.3	3.99	<i>Appl. Catal. B Environ.</i> , 2021, 299, 120656
11	F-FeNC-2	0.60	0.83	~3.7 (900 rpm)	3.98	<i>Mater. Horiz.</i> , 2022, 9, 417-424
12	Fe/Bi-RNC	~0.51	0.76	5.8	3.89	<i>J. Mater. Chem. A</i> , 2022, 10, 664-671
13	Fe-N-C-CeO ₂	0.60	0.80	~6.0	3.95	<i>Adv. Mater. Interfaces</i> , 2022, 9, 2200852
14	Fe@MNC-OAc	0.80	0.838	4.5 (900 rpm)	3.99	<i>Appl. Catal. B Environ.</i> , 2023, 324, 122209
15	Fe@G-800/100	0.294	0.70	~4.0	3.68	<i>ACS Sustain. Chem. Eng.</i> , 2023, 11, 21,

						8131–8139
16	FeNC@PM	0.50	0.78	5.12	3.90	This work